ICASSP 2023 - 2023 IEEE International Conference on Acoustics, Speech and Signal Processing (ICASSP) | 978-1-7281-6327-7/23/$31.00 ©2023 IEEE | DOI: 10.1109/ICASSP49357.2023.10094643

JOINT MILLIMETER-WAVE AOD AND AOA ESTIMATION USING ONE OFDM SYMBOL AND FREQUENCY-DEPENDENT BEAMS

Veljko Boljanovic and Danijela Cabric

University of California, Los Angeles
Electrical and Computer Engineering Department
vboljanovic@ucla.edu, danijela@ee.ucla.edu

ABSTRACT

When conventional phase shifter based arrays are used in millimeter-wave systems, the angle of departure (AoD) and angle of arrival (AoA) estimates are obtained through high-overhead exhaustive beam sweeping (EBS). Recently, true-time-delay arrays re-emerged as a promising architecture for fast angle estimation. In this work, we develop an algorithm for joint AoD and AoA estimation using only one Orthogonal Frequency Division Multiplexing (OFDM) symbol and frequency-dependent beams that can be synthesized by fully digital and true-time-delay arrays. We compare the developed algorithm with wideband single-carrier based EBS in terms of the misalignment probability and required training overhead. Numerical simulations in millimeter-wave channels reveal the advantages of the proposed algorithm.

***Index Terms*—** Millimeter-wave, AoD/AoA estimation, beam training, frequency-dependent beams, TTD array

1. INTRODUCTION

A common way to establish a directional link between the base station (BS) and user equipment (UE) in millimeter-wave (mmW) networks is through *beam training* [1], a procedure that identifies the dominant AoD and AoA, i.e., the best pair of steering directions. With large antenna arrays and narrow beams at the BS and UE, finding the optimal pair of angles, but keeping the training overhead and computational complexity low, is an important and challenging task.

Early work on fifth generation (5G) mmW communications usually assumed that the BS and UE have analog phased arrays, which can synthesize only one steering/combining beam at the time. For this reason, the existing beam training approaches for phased arrays include different variations of the EBS [2–4]. The main problem of sweeping is a large training overhead, which increases linearly with the number of antenna elements.

Previous work that addressed the problem of large beam training overhead can be roughly divided into two groups. The first group of works intend to leverage digital signal processing (DSP) techniques, such as compressive sensing, to reduce the required number of training symbols [5–7]. The second group of works aim to speed up angle estimation by using different array architectures, including digital arrays [8,9] and hybrid analog-digital arrays [10–12]. These arrays can use multiple radio frequency (RF) chains to design adaptive sector beams for hierarchical AoD and AoA estimation and/or to probe more than one angular direction at the time.

In an effort to minimize the required overhead, recent work proposed the use of true-time-delay arrays for angle estimation using a single OFDM symbol [13, 14]. Compared to phased arrays, true-time-delay (TTD) arrays have delay elements along with phase shifters in all antenna branches, which allow them to synthesize frequency-dependent (subcarrier-dependent) beams [15]. Thus, the information of the dominant propagation angle can be extracted from the subcarrier with the highest received signal power [13]. However, the training algorithms in [13–15] were mainly focused on AoA estimation at the UE side. In addition, previous work has not demonstrated the benefits of the single-symbol OFDM-based beam training over the conventional fast single-carrier based EBS. In this work, we address these problems. We first develop an algorithm for a *joint* AoD and AoA estimation that uses only one OFDM symbol and frequency-dependent beams. Then we compare the developed algorithm with single-carrier based EBS in terms of the misalignment probability and required training overhead.

This work was supported by the NSF under grant 1955672.

2. SYSTEM MODEL

We consider downlink beam training between the BS and UE using only one OFDM symbol. The carrier frequency, bandwidth, and number of subcarriers are denoted as f_c, BW, and M_tot, respectively. The OFDM symbol uses M ($M \leq M_\mathrm{tot}$) subcarriers from the predefined set $\mathcal{M}$, all loaded with binary phase shift keying (BPSK) modulated pilots. We assume that the BS is equipped with a fully digital antenna array [16], while the UE is assumed to be equipped with a fully connected hybrid TTD array with N_RF RF chains.

In this work, we consider a frequency-selective mmW channel with L multipath clusters. The channel matrix $\mathbf{H}[m] \in \mathbb{C}^{N_{\mathrm{R}} \times N_{\mathrm{T}}}$ at the m-th subcarrier is defined as

$$\mathbf{H}[m] = \sum_{l=1}^{L} g_l[m] \mathbf{a}_{\mathrm{R}}(\theta_l^{(\mathrm{R})}) \mathbf{a}_{\mathrm{T}}^{\mathrm{H}}(\theta_l^{(\mathrm{T})}), \tag{1}$$

where $g_l[m]$, $\theta_l^{(\mathrm{T})}$, and $\theta_l^{(\mathrm{R})}$ are a complex gain, AoD, AoA of the l-th cluster, respectively.

Let $\mathbf{v}[m] \in \mathbb{C}^{N_{\mathrm{T}}}$ be the BS digital precoder for the m-th subcarrier. Given (1), the received signal $y_r[m]$ at the m-th subcarrier in the r-th RF chain can be expressed as

$$y_r[m] = \mathbf{w}_r^{\mathrm{H}}[m]\mathbf{H}[m]\mathbf{v}[m]s[m] + \mathbf{w}_r^{\mathrm{H}}[m]\mathbf{n}[m],\ m \in \mathcal{M}, \tag{2}$$

where $\mathbf{w}_r[m] \in \mathbb{C}^{N_{\mathrm{R}}}$ is the UE analog TTD combiner for the m-th subcarrier in the r-th RF chain, $s[m]$ is a BPSK pilot at the m-th subcarrier, and $\mathbf{n}[m] \sim \mathcal{CN}\left(0, \sigma_{\mathrm{N}}^2 \mathbf{I}_{N_{\mathrm{R}}}\right)$ is white Gaussian noise. The n-th element of $\mathbf{w}_r[m]$ is $[\mathbf{w}_r[m]]_n = \exp\left[-j\left(2\pi(f_m - f_{\mathrm{c}})\tau_n + \phi_{r,n}\right)\right]$, where τ_n is the delay tap in the n-th antenna and $\phi_{r,n}$ is the phase tap in the n-th antenna and r-th RF chain. The frequency f_m of the m-th subcarrier is $f_m = f_{\mathrm{c}} - \mathrm{BW}/2 + (m-1)\mathrm{BW}/(M_{\text{tot}} - 1)$.

3. SINGLE-SYMBOL ANGLE ESTIMATION

3.1. Design of Beam Training Codebooks

Unlike in the UE-only beam training in [13, 14], joint AoD and AoA estimation requires frequency-dependent codebooks to be designed both at the BS and UE side. There are $N_{\mathrm{T}}N_{\mathrm{R}}$ beam pairs that need to be considered in the training. The key codebook design idea is to map OFDM subcarriers into different beam pairs. Thus, the set of used subcarriers $\mathcal{M}$ has $M = N_{\mathrm{T}}N_{\mathrm{R}}$ elements. The total of M_{tot} subcarriers is divided into N_{R} groups, and in each group, the first N_{T} subcarriers are selected and loaded with BPSK pilots. Mathematically, the set $\mathcal{M}$ is defined as $\mathcal{M} = \Big\{ m \mid m = m_{\mathrm{T}} + (m_{\mathrm{R}} - 1)\lfloor M_{\text{tot}}/(N_{\mathrm{R}})\rfloor,\ m_{\mathrm{T}} = 1, \cdots, N_{\mathrm{T}},\ m_{\mathrm{R}} = 1, \cdots, N_{\mathrm{R}} \Big\}$, where $\lfloor x \rfloor$ rounds x to the nearest lower integer. At the BS side, we design a codebook where in each of the N_{R} groups, the N_{T} subcarriers are assigned N_{T} different discrete Fourier transform (DFT) precoders $\mathbf{u}_{m_{\mathrm{T}}},\ m_{\mathrm{T}} = 1, ..., N_{\mathrm{T}}$, that cover the entire angular range $(-\pi/2, \pi/2)$. Equivalently, the subcarriers from the set $\mathcal{M}_{m_{\mathrm{T}}}^{(\mathrm{T})} = \{m \mid m = m_{\mathrm{T}} + (m_{\mathrm{R}} - 1)\lfloor M_{\text{tot}}/(N_{\mathrm{R}})\rfloor,\ m_{\mathrm{R}} = 1, ..., N_{\mathrm{R}}\}$ are assigned the m_{T}-th DFT precoder, i.e, $\mathbf{v}[m] = \mathbf{u}_{m_{\mathrm{T}}},\ m \in \mathcal{M}_{m_{\mathrm{T}}}^{(\mathrm{T})}$. At the UE side, we focus on the first RF chain and design a codebook where the N_{T} subcarriers from the set $\mathcal{M}_{m_{\mathrm{R}}}^{(\mathrm{R})} = \{m \mid m = m_{\mathrm{T}} + (m_{\mathrm{R}} - 1)\lfloor M_{\text{tot}}/(N_{\mathrm{R}})\rfloor,\ m_{\mathrm{T}} = 1, ..., N_{\mathrm{T}}\}$ are assigned the same DFT combiner $\mathbf{f}_{m_{\mathrm{R}}}$, i.e., $\mathbf{w}_1[m] = \mathbf{f}_{m_{\mathrm{R}}},\ m \in \mathcal{M}_{m_{\mathrm{R}}}^{(\mathrm{R})}$. The design of training codebooks is illustrated on a small example in Fig. 1.

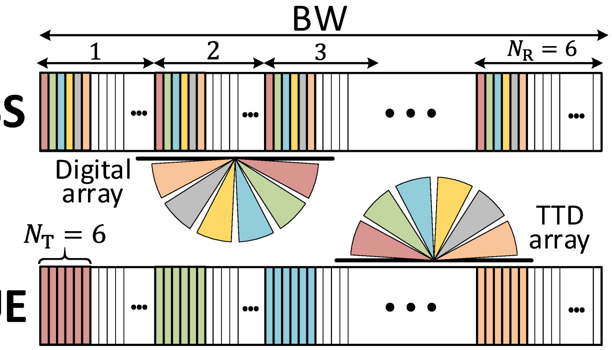

Fig. 1. Illustration of subcarrier selection and codebook design at the BS and UE, assuming $N_{\mathrm{T}} = 6$ and $N_{\mathrm{R}} = 6$.

Since the BS is equipped with a digital array, its codebook can be easily designed through the frequency-domain DSP. On the other hand, the UE codebook is created by setting the delay taps $\tau_n,\ \forall n$, and phase taps $\phi_{r,n},\ \forall r, n$. Similarly as in [13], we set the delay taps to be $\tau_n = (n-1)/\mathrm{BW},\ 1 \le n \le N_{\mathrm{R}}$, to probe all AoAs in the range $(-\pi/2, \pi/2)$. The N_{T} subcarriers from the set $\mathcal{M}_{m_{\mathrm{R}}}^{(\mathrm{R})}$ correspond to different frequencies and thus they experience slightly different combining angles and beamforming gains. The difference in beamforming gains is reduced by using the phase shifters to align the UE codebook. The alignment phase tap is the same in all RF chains and for the n-th antenna it is given as $\phi_{\text{al},n} = -(n-1)\mathrm{mod}\left(2\pi(f_{\text{mid}} - f_{\mathrm{c}})/\mathrm{BW} + \pi, 2\pi\right)$, where $f_{\text{mid}} = f_{N_{\mathrm{T}}/2} + \mathrm{BW}/(2M_{\text{tot}} - 2)$ is the "middle" frequency of the subcarriers in $\mathcal{M}_1^{(\mathrm{R})}$ and mod() is the modulo operator. To increase the robustness to frequency-selective channels through frequency diversity, we rotate the UE codebook in different RF chains by using the rotation phase taps $\phi_{\text{rot},r,n} = (r-1)(n-1)2\lfloor N_{\mathrm{R}}/N_{\mathrm{RF}}\rfloor\pi/N_{\mathrm{R}},\ \ \forall r, n$. These taps ensure that the codebook diversity is $R = N_{\mathrm{RF}}$, i.e., that each AoD-AoA beam pair is probed by N_{RF} different subcarriers in different RF chains. Thus, the overall phase taps are set as $\phi_{r,n} = \phi_{\text{al},n} + \phi_{\text{rot},r,n},\ \ 1 \le r \le N_{\mathrm{RF}}, 1 \le n \le N_{\mathrm{R}}$.

3.2. Design of DSP Algorithm for Beam Training

We use the designed BS and UE beam training codebooks to develop a DSP algorithm for joint AoD and AoA estimation. We propose a non-coherent power-based algorithm that does not rely on phase information in samples in (2). We also consider a coherent power-based algorithm and include it in the analysis of the misalignment probability as the benchmark.

Let b be the index of the beam pair defined by the precoder $\mathbf{u}_{m_{\mathrm{T}}}$ and combiner $\mathbf{f}_{m_{\mathrm{R}}}$. We define the set of $R = N_{\mathrm{RF}}$ subcarriers that probe the b-th beam pair as $\mathcal{M}_b^{(\mathrm{B})} = \Big\{ m | m = \mathrm{mod}\left(m_b + (r-1)\left\lfloor \frac{N_{\mathrm{R}}}{N_{\mathrm{RF}}}\right\rfloor \left\lfloor \frac{M_{\text{tot}}}{N_{\mathrm{R}}}\right\rfloor,\ M\right),\ r = 1, ..., R \Big\}$.

We vectorize the transmitted symbols $s[m],\ \forall m \in \mathcal{M}_b^{(\mathrm{B})}$ for the beam pair b and we denote the resulting vector $\mathbf{s}_b$. Similarly, we vectorize the corresponding received signal samples $y_r[m],\ \forall(r,m), m \in \mathcal{M}_b^{(\mathrm{B})}$, and we denote that vector $\mathbf{y}_b \in \mathbb{C}^{N_{\mathrm{RF}}}$. A non-coherent power measurement $\hat{p}_b^{(\mathrm{nc})}$ for the beam pair b is then defined as follows

$$\hat{p}_b^{(\mathrm{nc})} = \frac{2}{\sigma_{\mathrm{N}}^2}\mathbf{y}_b^{\mathrm{H}}\mathbf{y}_b = \frac{2}{\sigma_{\mathrm{N}}^2}\sum_{(r,m),m\in\mathcal{M}_b^{(\mathrm{B})}} |y_r[m]|^2, \qquad (3)$$

where $2/\sigma_{\mathrm{N}}^2$ is the scaling term. Note that $\hat{p}_b^{(\mathrm{nc})}$ includes powers of R frequency-domain samples (subcarriers). On the other hand, a benchmark coherent measurement $\hat{p}_b^{(\mathrm{c})}$, which requires complex synchronization, is defined as $\hat{p}_b^{(\mathrm{c})} = \frac{2}{\|\mathbf{s}_b\|_2^2\sigma_{\mathrm{N}}^2}|\mathbf{y}_b^{\mathrm{H}}\mathbf{s}_b|^2$, where $2/(\|\mathbf{s}_b\|_2^2\,\sigma_{\mathrm{N}}^2)$ is the scaling term. Coherent power measurements were previously studied in [17].

The AoD and AoA estimates are based on the beam pair index $\hat{b}_{\max}^{(\mathrm{nc})}$ that corresponds to the maximum measured power $\hat{p}_{\max}^{(\mathrm{nc})}$. The values of $\hat{p}_{\max}^{(\mathrm{nc})}$ and $\hat{b}_{\max}^{(\mathrm{nc})}$ are found as follows

$$\hat{p}_{\max}^{(\mathrm{nc})} = \max_{\hat{p}_b^{(\mathrm{nc})}} \hat{p}_b^{(\mathrm{nc})}, \quad \hat{b}_{\max}^{(\mathrm{nc})} = \operatorname*{argmax}_b \hat{p}_b^{(\mathrm{nc})}. \qquad (4)$$

Let $\xi_{m_{\mathrm{T}}^*}^{(\mathrm{T})}$ and $\xi_{m_{\mathrm{R}}^*}^{(\mathrm{R})}$ be the steering angles that correspond to $\hat{b}_{\max}^{(\mathrm{nc})}$. Then the on-grid AoD and AoA estimates are

$$\hat{\theta}^{(\mathrm{T})} = \xi_{m_{\mathrm{T}}^*}^{(\mathrm{T})}, \quad \hat{\theta}^{(\mathrm{R})} = \xi_{m_{\mathrm{R}}^*}^{(\mathrm{R})}. \qquad (5)$$

3.3. Misalignment Probability in Presence of Noise

In low signal-to-noise ratios (SNR), the performance of beam training algorithms can be affected by noise. In [17], the authors studied the beam pair misalignment probability in the presence of Gaussian noise in the single-carrier based EBS with coherent power measurements. The same methodology can be used to analyze the misalignment probability $P_{\mathrm{miss}}^{(\mathrm{nc})}$ in the proposed single-symbol OFDM-based beam training, where non-coherent power measurements are made in the frequency-domain.

Without loss of generality, let the index $b=1$ correspond to the optimal beam pair with the maximum received power, i.e., $p_{\max}^{(\mathrm{nc})} = p_1^{(\mathrm{nc})}$. Then, following the derivation in [17], the upper bound on the beam pair misalignment probability is $P_{\mathrm{up}}^{(\mathrm{nc})} = \sum_{b=2}^{M}\mathbb{P}[\hat{p}_1^{(\mathrm{nc})}/\hat{p}_b^{(\mathrm{nc})} < 1]$. The ratio $\hat{p}_1^{(\mathrm{nc})}/\hat{p}_b^{(\mathrm{nc})}$ of two non-central chi-squared random variables is a random variable with a doubly non-central F distribution, denoted as $F(n_1,n_2,\eta_1,\eta_2)$. Thus, the upper bound $P_{\mathrm{up}}^{(\mathrm{nc})}$ is [17]

$$P_{\mathrm{up}}^{(\mathrm{nc})} = \sum_{b=2}^{M} F(1|n_1,n_1,\eta_1,\eta_b), \qquad (6)$$

where $n_1 = 2R$, $n_2 = 2R$, $\eta_b = \frac{2}{\sigma_{\mathrm{N}}^2}\frac{1}{M}\sum_{(r,m)\in\mathcal{M}_b^{(\mathrm{B})}} |\mathbf{w}_r^H[m]\mathbf{H}[m]\mathbf{v}[m]|^2,\ b=1,...,M$.

In the next section, we compare the proposed beam training with the single-carrier based EBS. The comparison is done in terms of the SNR per sample, misalignment probability, and required overhead.

4. COMPARISON WITH EBS

In this section, we compare the single-symbol OFDM-based beam training with fast single-carrier based EBS, and we we demonstrate the benefits of the proposed approach.

We first compare the proposed beam training and EBS in terms of the SNR per sample. In the proposed OFDM-based beam training, the measurements include powers of R samples from different subcarriers. Based on the system model, the SNR per sample is $\mathrm{SNR} = 1/(M\sigma_{\mathrm{N}}^2)$. Conversely, in the single-carrier based EBS, power measurements are made across multiple time-domain samples (symbols) and the entire bandwidth is used for each sample. Thus, the SNR per sample can be expressed as $\mathrm{SNR} = \mathrm{BW}_{\mathrm{TTD}}/(M_{\mathrm{tot}}\sigma_{\mathrm{N}}^2\mathrm{BW}_{\mathrm{EBS}})$, where the ratio $\mathrm{BW}_{\mathrm{TTD}}/\mathrm{BW}_{\mathrm{EBS}}$ accounts for a potential difference in the bandwidths used in the proposed beam training and EBS. Clearly, if $\mathrm{BW}_{\mathrm{TTD}} = \mathrm{BW}_{\mathrm{EBS}}$, the proposed OFDM-based beam training has M_{tot}/M times larger SNR per sample that the single-carrier based EBS.

Next, we compare the two approaches in terms of the beam pair misalignment probability in a simple line-of-sight (LoS) channel. For simplicity, all beams are assumed to have a uniform beamforming gain. We use the following parameters: $N_{\mathrm{T}} = 32$, $N_{\mathrm{R}} = 16$, $\mathrm{BW}_{\mathrm{TTD}} = \mathrm{BW}_{\mathrm{EBS}} = 1$ GHz, $M_{\mathrm{tot}} = 4096$, $M = 512$, $\mathrm{SNR} = -22$ dB (before beamforming in proposed approach). It is assumed that the total duration of all transmitted symbols is the same in both approaches and it is equal to $M_{\mathrm{tot}}/\mathrm{BW}$ (one OFDM symbol without cyclic prefix). With such total duration and $R = N_{\mathrm{RF}}$, the number of samples per beam pair power measurement is R and RM_{tot}/M in the proposed beam training and single-carrier based EBS, respectively. The misalignment probability is presented in Fig. 2 as a function of the number of RF chains N_{RF}. We present both the simulated curves and the calculated upper bounds. The results indicate that the coherent power measurements lead to a lower misalignment probability than non-coherent power measurements in both the proposed beam training and EBS. Additionally, the proposed beam training is shown to have the same misalignment probability as the EBS when coherent power measurements are used in simple LoS channels. However, when non-coherent power measurements are used, the proposed joint beam training outperforms the EBS. The main reason for this is a higher SNR per sample in the proposed beam training with an OFDM waveform and frequency-dependent beams. Similar as in energy detection algorithms in spectrum sensing, the required number of samples in non-coherent beam training highly depends on the SNR. Thus, the EBS needs more samples to achieve the same misalignment probability

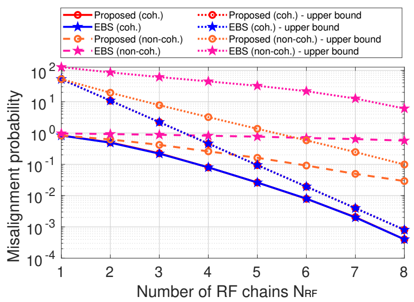

Fig. 2. Misalignment probability in a simple LoS channel.

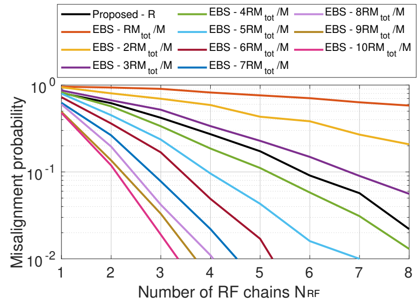

Fig. 3. Misalignment probability in the EBS when more samples are used.

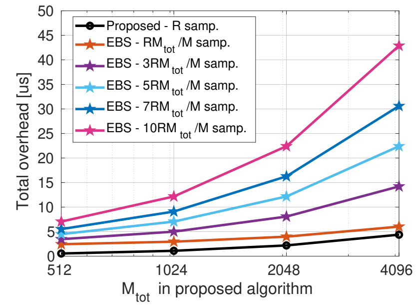

Fig. 4. Total required overhead for beam training.

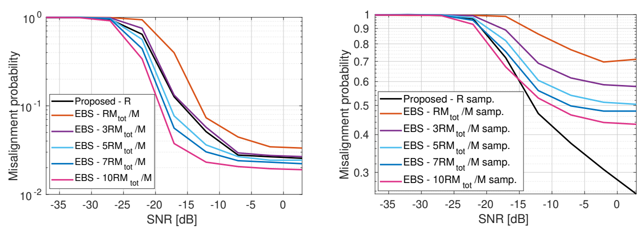

(a) (b)

Fig. 5. Mis. prob. in realistic (a) LoS and (b) NLoS channels.

as the proposed beam training, numerically studied in Fig. 3. The simulated curves in Fig. 3 indicate that the EBS needs an $N_{\mathrm{S}} = 3$ times or $N_{\mathrm{S}} = 4$ times higher number of samples for a comparable performance.

One of the main advantages of the proposed beam training over the fast single-carrier based EBS is a lower total required overhead. The overhead in the proposed beam training is equivalent to the duration of a single OFDM symbol, which is $T_{\mathrm{TTD}} = 1.07 M_{\mathrm{tot}}/\mathrm{BW}_{\mathrm{TTD}}$, assuming a 7% cyclic prefix. On the other hand, the overhead of the EBS depends on the total duration of transmitted single-carrier symbols. During the one OFDM symbol in the proposed beam training, a total of $M_{\mathrm{tot}}\mathrm{BW}_{\mathrm{EBS}}/\mathrm{BW}_{\mathrm{TTD}}$ single-carrier symbols are transmitted in the EBS. However, as discussed earlier, the EBS needs to increase the number of symbols (samples) to achieve the same performance as the proposed beam training. In addition, the EBS requires the BS and UE to set up and switch the beams for each probed beam pair. Since the BS is equipped with a digital array, its beam can be set up and switched in DSP. On the other hand, the hybrid array at the UE needs to reconfigure its phase shifters when a different receive beam is probed. Thus, the total training overhead in the EBS can be expressed as $T_{\mathrm{EBS}} = N_{\mathrm{S}} M_{\mathrm{tot}} 1/\mathrm{BW}_{\mathrm{TTD}} + N_{\mathrm{R}}(T_{\mathrm{setup}} + T_{\mathrm{switch}})$, where T_{setup} and T_{switch} are the set up and switching times. In the state-of-the-art antenna arrays, these values are around $T_{\mathrm{setup}} = 120$ ns and $T_{\mathrm{switch}} = 8$ ns [18]. We evaluated the total training overhead in the proposed beam training and EBS in Fig. 4. The results confirm that the proposed beam training has a significantly lower overhead than the EBS.

Finally, we evaluate the misalignment probability in the proposed beam training algorithm and EBS in realistic LoS and non-line-of-sight (NLoS) mmW channels generated in Quadriga [19]. In these simulations, we do not use the simplifying assumption that all beams have a uniform beamforming gain. The results are presented in Fig. 5. Similar as in the simplified LoS channel, the EBS requires a larger number of samples to achieve the same performance as the proposed beam training in realistic LoS channels. Without the assumption of uniform beamforming gains, the misalignment probability experiences a floor in high SNR in both approaches. Nevertheless, the probability floor is still fairly low, in the order of 10^{-2}. Unlike in LoS channels, there are multiple comparably strong propagation clusters in NLoS channels and it is easier to miss the optimal beam pair, even in high SNRs. Thus, the floor beam pair misalignment probability is higher in NLoS than in LoS channels for both the proposed beam training and EBS. In addition, NLoS channels have significantly larger delay spreads than LoS channels. The proposed beam training, which uses a long OFDM waveform, is resistant to inter-symbol interference and it can capture the entire energy of NLoS channels with large delay spreads. On the other hand, short symbols in the single-carrier based EBS are susceptible to inter-symbol interference and they cannot capture the time-spread channel energy. This leads to a lower received signal power and a higher misalignment probability in the EBS. The performance gap between the two approaches can be reduced by increasing the number of samples, and thus the total overhead, in the EBS.

5. CONCLUSIONS

In this work, we proposed a beam training algorithm for fast joint AoD and AoA estimation. With a proper design of frequency-dependent codebooks and a simple DSP algorithm, angle estimates can be acquired using only one OFDM symbol. The results indicate that the proposed algorithm leads to a lower misalignment probability and required beam training overhead than the conventional single-carrier based EBS.

6. REFERENCES

[1] R. W. Heath, N. González-Prelcic, S. Rangan, W. Roh, and A. M. Sayeed, "An overview of signal processing techniques for millimeter wave MIMO systems," *IEEE Journal of Selected Topics in Signal Processing*, vol. 10, no. 3, pp. 436–453, Apr. 2016.

[2] C. Jeong, J. Park, and H. Yu, "Random access in millimeter-wave beamforming cellular networks: issues and approaches," *IEEE Communications Magazine*, vol. 53, no. 1, pp. 180–185, 2015.

[3] C. Liu, M. Li, L. Zhao, P. Whiting, S. V. Hanly, and I. B. Collings, "Millimeter-wave beam search with iterative deactivation and beam shifting," *IEEE Transactions on Wireless Communications*, vol. 19, no. 8, pp. 5117–5131, 2020.

[4] A. K. R. Chavva and N. B. Mehta, "Millimeter-wave beam selection in time-varying channels with user orientation changes," *IEEE Transactions on Wireless Communications*, vol. 20, no. 11, pp. 6987–7000, 2021.

[5] H. Yan and D. Cabric, "Compressive initial access and beamforming training for millimeter-wave cellular systems," *IEEE Journal of Selected Topics in Signal Processing*, vol. 13, no. 5, pp. 1151–1166, 2019.

[6] M. Bajor, T. Haque, G. Han, C. Zhang, J. Wright, and P. R. Kinget, "A flexible phased-array architecture for reception and rapid direction-of-arrival finding utilizing pseudo-random antenna weight modulation and compressive sampling," *IEEE Journal of Solid-State Circuits*, vol. 54, no. 5, pp. 1315–1328, 2019.

[7] M. E. Rasekh, Z. Marzi, Y. Zhu, U. Madhow, and H. Zheng, "Noncoherent mmWave path tracking," in *Proceedings of the 18th International Workshop on Mobile Computing Systems and Applications*, New York, NY, USA, 2017, HotMobile '17, p. 13–18, Association for Computing Machinery.

[8] V. Desai, L. Krzymien, P. Sartori, W. Xiao, A. Soong, and A. Alkhateeb, "Initial beamforming for mmWave communications," in *2014 48th Asilomar Conference on Signals, Systems and Computers*, 2014, pp. 1926–1930.

[9] C. N. Barati, S. A. Hosseini, M. Mezzavilla, T. Korakis, S. S. Panwar, S. Rangan, and M. Zorzi, "Initial access in millimeter wave cellular systems," *IEEE Transactions on Wireless Communications*, vol. 15, no. 12, pp. 7926–7940, 2016.

[10] A. Alkhateeb, O. El Ayach, G. Leus, and R. W. Heath, "Channel estimation and hybrid precoding for millimeter wave cellular systems," *IEEE Journal of Selected Topics in Signal Processing*, vol. 8, no. 5, pp. 831–846, 2014.

[11] D. De Donno, J. Palacios, and J. Widmer, "Millimeter-wave beam training acceleration through low-complexity hybrid transceivers," *IEEE Transactions on Wireless Communications*, vol. 16, no. 6, pp. 3646–3660, 2017.

[12] S. Noh, M. D. Zoltowski, and D. J. Love, "Multi-resolution codebook and adaptive beamforming sequence design for millimeter wave beam alignment," *IEEE Transactions on Wireless Communications*, vol. 16, no. 9, pp. 5689–5701, 2017.

[13] H. Yan, V. Boljanovic, and D. Cabric, "Wideband millimeter-wave beam training with true-time-delay array architecture," in *2019 53rd Asilomar Conference on Signals, Systems, and Computers*, 2019, pp. 1447–1452.

[14] V. Boljanovic, H. Yan, C. C. Lin, S. Mohapatra, D. Heo, S. Gupta, and D. Cabric, "Fast beam training with true-time-delay arrays in wideband millimeter-wave systems," *IEEE Transactions on Circuits and Systems I: Regular Papers*, vol. 68, no. 4, pp. 1727–1739, 2021.

[15] C. Jans, X. Song, W. Rave, and G. Fettweis, "Frequency-selective analog beam probing for millimeter wave communication systems," in *2020 IEEE Wireless Communications and Networking Conference (WCNC)*, 2020, pp. 1–6.

[16] H. Yan, S. Ramesh, T. Gallagher, C. Ling, and D. Cabric, "Performance, power, and area design trade-offs in millimeter-wave transmitter beamforming architectures," *IEEE Circuits and Systems Magazine*, vol. 19, no. 2, pp. 33–58, 2019.

[17] C. Liu, M. Li, S. V. Hanly, I. B. Collings, and P. Whiting, "Millimeter wave beam alignment: Large deviations analysis and design insights," *IEEE Journal on Selected Areas in Communications*, vol. 35, no. 7, pp. 1619–1631, 2017.

[18] B. Sadhu, A. Paidimarri, W. Lee, M. Yeck, C. Ozdag, Y. Tojo, J.-O. Plouchart, X. Gu, Y. Uemichi, S. Chakraborty, Y. Yamaguchi, N. Guan, and A. Valdes-Garcia, "A 24-to-30GHz 256-element dual-polarized 5G phased array with fast beam-switching support for ¿30,000 beams," in *2022 IEEE International Solid-State Circuits Conference (ISSCC)*, 2022, vol. 65, pp. 436–438.

[19] S. Jaeckel, L. Raschkowski, K. Börner, L. Thiele, F. Burkhardt, and E. Eberlein, "QuaDRiGa - Quasi Deterministic Radio Channel Generator, user manual and documentation," *Fraunhofer Heinrich Hertz Institute, Tech. Rep. v2.2.0*, 2019.